Evaluating two concepts for the modelling of intermediates accumulation during biological denitrification in wastewater treatment

Yuting Pan[1], Bing-Jie Ni[1], Huijie Lu[2], Kartik Chandran[3], David Richardson[1,4], Zhiguo Yuan[1]*

[1]Advanced Water Management Centre (AWMC), The University of Queensland, St Lucia, Brisbane, QLD 4072, Australia

[2]Department of Civil and Environmental Engineering, University of Vermont, Burlington, VT 05405, USA

[3]Department of Earth and Environmental Engineering, Columbia University, New York, NY 10027, USA

[4]Centre for Molecular Structure and Biochemistry (CMSB), School of Biological Sciences, University of East Anglia, Norwich, NR4 7TJ, UK

* Corresponding author: phone + 61 7 3365 4374; fax +61 7 3365 4726; email: zhiguo@awmc.uq.edu.au

ABSTRACT

The accumulation of the denitrification intermediates in wastewater treatment systems is highly undesirable, since both nitrite and nitric oxide (NO) are known to be toxic to bacteria, and nitrous oxide (N_2O) is a potent greenhouse gas and an ozone depleting substance. To date,

two distinct concepts for the modelling of denitrification have been proposed, which are represented by the Activated Sludge Model for Nitrogen (ASMN) and the Activated Sludge Model with Indirect Coupling of Electrons (ASM-ICE), respectively. The two models are fundamentally different in describing the electron allocation among different steps of denitrification. In this study, the two models were examined and compared in their ability to predict the accumulation of denitrification intermediates reported in four different experimental datasets in literature. The N-oxide accumulation predicted by the ASM-ICE model was in good agreement with values measured in all four cases, while the ASMN model was only able to reproduce one of the four cases. The better performance of the ASM-ICE model is due to that it adopts an "indirect coupling" modelling concept through electron carriers to link the carbon oxidation and the nitrogen reduction processes, which describes the electron competition well. The ASMN model, on the other hand, is inherently limited by its structural deficiency in assuming that carbon oxidation is always able to meet the electron demand by all denitrification steps, therefore discounting electron competition among these steps. ASM-ICE therefore offers a better tool for predicting and understanding intermediates accumulation in biological denitrification.

Key words: denitrification modelling, electron competition, carbon source, nitrous oxide, ASMN, ASM-ICE

1. INTRODUCTION

Denitrification is an important process of the global nitrogen cycle. Nitrate reduction consists of four consecutive reduction steps, with nitrite (NO_2^-), nitric oxide (NO) and nitrous oxide (N_2O) as three obligatory intermediates (Zumft 1997). Each reduction step is catalysed by one or more specific enzymes, including nitrate reductase (Nar), nitrite reductase (Nir), NO

reductase (Nor) and N_2O reductase (Nos). In wastewater treatment systems, denitrification, together with nitrification, are the key processes to remove nitrogen pollutants from wastewater (Tchobanoglous et al. 2003).

A long-existing operational issue of wastewater denitrification is the accumulation of N-oxide intermediates. Nitrite and NO are known to be toxic, which could suppress the activity of denitrifiers (Zumft 1997, Ni and Yu 2008). In recent years, the emission of nitrous oxide from wastewater treatment plants (WWTPs) has become an emerging problem, because N_2O is a potent greenhouse gas with a 300-fold stronger radiative force than carbon dioxide, and is also a primary ozone depleting substance in the 21 century (IPCC 2007, Ravishankara et al. 2009).

It has been demonstrated that the accumulation of denitrification intermediates is often a result of electron competition among N-reductases involved in the four denitrification steps (Pan et al. 2013a, Schalk-Otte et al. 2000). Pure culture-based studies of electron transport network in typical denitrifying bacteria, such as *Paracoccus denitrificans*, have proven that all denitrification enzymes derive their electrons from a common electron supply source, i.e., the ubiquinol pool of the respiratory electron transport chain (Richardson et al. 2009). The structure of this electron transport network sets the stage for the electron competition between the four denitrification steps. The electron competition occurs when the electron supply rate is rate-limiting during denitrification.

Mathematical modelling has been widely applied to predict nitrogen removal in wastewater treatment. Previous modelling efforts have primarily focussed on the prediction of nitrate removal (Henze et al. 2000), and in some cases, nitrite as well (Ni and Yu 2008). However, it

is increasingly recognised that N_2O accumulation should also be modelled, especially due to its detrimental influence on the atmosphere (Ni et al. 2011). It has been proposed to achieve this goal through modelling denitrification as a four-step process, using NO_3^-, NO_2^-, NO, and N_2O as the terminal electron acceptor, respectively (Vonschulthess et al. 1994, Schulthess and Gujer 1996, Hiatt and Grady 2008, Pan et al. 2013b). With each step being modelled with individual, reaction-specific kinetics, the accumulation of nitrite, NO and N_2O can be predicted.

To date, two distinct concepts have been proposed for modelling the four-step denitrification, with their structures shown in Figure 1.

Model I*: The "direct coupling approach",* represented by Activated Sludge Model for Nitrogen (ASMN) (Hiatt and Grady 2008), in which the carbon oxidation and nitrogen reduction processes are directly coupled. This type of model describes each of the four steps as a separate and independent oxidation-reduction reaction (Figure 1-a), and reaction-specific kinetics are applied. Many of the multiple step denitrification models have adopted such structure (e.g., Ni et al. (2011), Schulthess and Gujer (1996).

Model II*: the "indirect coupling approach",* proposed by Pan et al. (2013a) and named Activated Sludge Model for Indirect Coupling of Electrons (ASM-ICE), in which the carbon oxidation and nitrogen reduction processes are indirectly coupled. Electron carriers are introduced as a new component in this model to link carbon oxidation to nitrogen oxides reduction (Figure 1-b). As a result, each step of denitrification can be regulated by both the nitrogen reduction and the carbon oxidation processes.

100 It is of importance to evaluate the abilities of these two models in predicting denitrification
101 activities and particularly the accumulation of denitrification intermediates. This can be done
102 by conducting parallel comparisons with existing data reported for different denitrifying
103 cultures and/or under different conditions. Therefore, the aim of this work is to reveal how
104 the two model structures presented in Figure 1 would affect their ability to reproduce
105 experimental data reported in literature. Four distinctive denitrifying cultures were used in
106 this examination, including one pure culture (*P. denitrijkans* (N.C.1.B. 8944)) and three
107 mixed denitrifying cultures/sludge fed with different substrates (e.g., acetate or methanol). In
108 particular, the ability of the two models in predicting electron competition during
109 denitrification was assessed. The findings are expected to improve the fundamental
110 understanding of electron competition involved in specific denitrification steps, which could
111 ultimately lead to better modelling and control of intermediate accumulation during
112 wastewater denitrification.
113
114 **2. MATERIALS AND METHODS**
115 **2.1. Mathematical models for denitrification**
116 The kinetic and stoichiometric matrices describing the nitrogen reduction and the carbon
117 oxidation processes for the two mathematical models are presented in Table 1. Nomenclature
118 for all state variables used in this article slightly differs from the original publications (Hiatt
119 and Grady 2008, Pan et al. 2013b). We employ the following symbols for concentrations of
120 various components: heterotrophic biomass (X), nitrate (S_{NO3}), nitrite (S_{NO2}), nitric oxide
121 (S_{NO}), nitrous oxide (S_{N2O}), readily biodegradable carbon source (S_s), reduced form of
122 electron carriers (S_{Mred}), oxidized form of electron carriers (S_{Mox}). Other processes involved
123 in denitrification, such as death and lysis of heterotrophs, hydrolysis of particulate organic
124 nitrogen, are included in both models with standard ASM kinetic expressions and parameter

125 values taken from published literature (Hiatt and Grady 2008). Table 2 lists the definitions,
126 values and units of the parameters used in the two models. Both models are based on mass
127 balance, but with different units. The ASMN model adopted weight unit (gram chemical
128 oxygen demand (COD) and g N) while the ASM-ICE model adopted mole units (mole COD
129 and mole N). The two sets of units can be easily converted.
130
131 As shown in Table 1, with the ASMN model (Model I), the reduction of nitrogen oxide
132 compounds (nitrate, nitrite, nitric oxide and nitrous oxide) and the oxidation of organic
133 carbon are "directly coupled" in a single oxidation-reduction reaction with a process
134 stoichiometry based on electron balance (i.e. I-R_1, I-R_2, I-R_3, I-R_4). In particular, the role of
135 carbon oxidation in denitrification is reflected through the following two aspects: 1) the
136 affinity constants for carbon source of each denitrification step (K_{S1}, K_{S2}, K_{S3}, K_{S4}) can be
137 different; 2) the overall carbon oxidation rate is modelled as the sum of the four
138 denitrification steps. The underlying assumption of this modelling approach is that carbon
139 oxidation is always able to meet the demand for electrons by all the four denitrification steps.
140 However, in reality, carbon oxidation could be the rate-limiting step, affecting the
141 denitrification steps through electron competition. The conceptual reaction schemes of the
142 ASMN model are detailed in the supplementary materials.
143
144 In contrast, in the ASM-ICE model (Model II), the carbon oxidation process (II-R_1) is
145 decoupled from the nitrogen reduction processes (II-R_2 to II-R_5). Electron carriers, with *Mox*
146 representing oxidized from of electron carriers and *Mred* ($Mred \leftrightharpoons Mox + 2e^- + 2H^+$)
147 representing reduced form of electron carriers, are introduced as new components in this
148 model to link the carbon oxidation process and the nitrogen oxides reduction processes. *Mox*
149 gains electrons from carbon oxidation and meanwhile being reduced to *Mred* (II-R_1), while

Mred donates electrons to nitrogen reduction and meanwhile being oxidized back to *Mox* (II-R_2 to II-R_5). The recirculation loop between *Mox* and *Mred* were realized in the ASM-ICE model by implementing $S_{Mred} + S_{Mox} = C_{tot}$, where C_{tot} is a constant value related to the total concentration of electron carriers. The relative ability of each denitrification step to compete for electrons determines the electron distribution, and consequentially the denitrification intermediate accumulation. The different values for the four affinity constants of each denitrification step with respect to electrons ($K_{Mred,1}$, $K_{Mred,2}$, $K_{Mred,3}$ and $K_{Mred,4}$) largely affect the competitiveness of different reduction steps for electrons when the overall carbon oxidation rate become rate limiting. SMox and SMred are the concentrations of electron carriers related to active biomass in the system. Therefore, they could be set to zero in influent, given the small amount of active biomass in influent wastewater. The conceptual reaction schemes of the ASM-ICE model are detailed in the supplementary materials.

2.2. Testing the predictive abilities of the models

Experimental data from four cases (Kucera et al. 1983, Pan et al. 2012, McMurray 2008, Oh and Silverstein 1999) studying denitrification intermediates dynamics were used to test the predictive abilities of the two mathematical models (Table 3).

Case 1 (Kucera et al. 1983): The branching of the electron flow to individual terminal acceptors NO_3^-, NO_2^- and N_2O was investigated in a pure denitrifying culture *Paracoccus denitrijkans* (N.C.1.B. 8944). The culture was cultivated anaerobically to early stationary phase. A closed reactor with magnetic stirrer was used to carry out batch tests, during which N_2 was provided into the reactor to ensure oxygen free environment. The reaction medium contained 0.25 M sucrose, 20mM Tris/sulphate at pH 7.3. At the beginning of the reaction, 50 mM glucose and 1 mM KNO_3 were added. Nitrate concentration was determined with a

175 nitrate-specific electrode. Nitrite concentration was determined colorimetrically. Nitric oxide
176 and N_2O were not measured in the experiment. Two sets of batch tests (*Set A* and *Set B*) were
177 conducted to assess the nitrate and nitrite reduction dynamics.
178
179 Two sets of batch tests (*Set A* and *Set B*) were conducted to assess the nitrate and nitrite
180 reduction dynamics.
181
182 • **In batch test *Set A***, nitrate was firstly added to reach a concentration of 14 mg N/L at the
183 beginning of the test, and then nitrite was added at 0.5 hour to reach around 5 mg N/L.
184 The reduction profiles of both nitrate and nitrite were monitored.
185 • **In batch test *Set B***, nitrate was firstly added to achieve a concentration ranging from 10
186 to 14 mg N/L at the beginning of each test, with the nitrate reduction profile being
187 monitored. Then, either 1) nitrite, or 2) N_2O, or 3) a mixture of nitrite, N_2O and antimycin
188 (an inhibitor for nitrite and N_2O reduction) were added. Therefore, the nitrate reduction
189 rate was measured under the following four different conditions: 1) with only NO_3^- as the
190 substrate; 2) with NO_3^- and NO_2^-; 3) with NO_3^- and N_2O; 4) with NO_3^-, antimycin, NO_2^-
191 and N_2O.
192
193 Case 2 (McMurray 2008): To investigate the denitrification intermediates dynamics, the
194 reduction of nitrate and nitrite, and the corresponding nitrogen gas production by a full-scale
195 activated sludge fed with acetate were studied. The activated sludge was collected from the
196 anoxic zone in a full-scale WWTP. All batch experiments were performed in a 2 litre, sealed
197 Perspex reactor fitted with pH (Ionode IJ44, TPS, Brisbane, Australia) and DO (YSI model
198 5739, Yellow Springs,USA) probes. The pH was maintained at 7.0 ± 0.01 throughout each
199 test, and temperature controlled at 22 °C. The nitrate and nitrite concentrations were analyzed

using a Lachat QuikChem8000 Flow Injection Analyzer (Lachat Instrument, Milwaukee, Wisconsin). The N_2 gas was monitored using a mass spectrometer. ” Nitric oxide and N_2O were not measured in the experiment.

At the beginning of the batch test, nitrate and nitrite were added to achieve initial concentrations around 5.2 mg N/L and 8.9 mg N/L, respectively. Acetate was also added at the same time, and was present in excess throughout the test. The conversions of nitrate, nitrite and acetate were monitored, along with the production rate of nitrogen gas (N_2).

Case 3 (Pan et al. 2013a): This study aimed to understand the electron competition process during denitrification, using an enriched denitrifying culture fed with methanol. Batch tests were performed in a 300 mL sealed reactor under anaerobic conditions. The pH was maintained at 8.0 ± 0.01 throughout each test. The batch tests were performed in a temperature-controlled room at 22.0 - 23.0°C. Methanol and various nitrogen oxides were supplied to the mixed liquor in each test. The nitrate and nitrite concentrations were analyzed using a Lachat QuikChem8000 Flow Injection Analyzer (Lachat Instrument, Milwaukee, Wisconsin). Methanol was analysed by gas chromatography (Perkin Elmer Autosystem). N_2O in the liquid phase was measured online using a N_2O microsensor (N_2O-100, Unisense A/S. Aarhus, Denmark).

Four batch tests reported therein are chosen in this paper to evaluate the two types of models, including 1) the reduction of NO_3^- with itself being added as the sole externally-supplied electron acceptor; 2) the reduction of NO_2^- with itself being added as the sole externally-supplied electron acceptor; 3) the reduction of N_2O with itself being added as the sole externally-supplied electron acceptor; 4) the reduction of NO_3^-, NO_2^- and N_2O with all of

them being added simultaneously. The initial concentrations of the nitrogen compounds were between 30 and 50 mg N/L. Methanol was used as the carbon source and was in excess in all these four tests. The reduction of the nitrogen compounds were monitored throughout the tests.

Case 4 (Oh and Silverstein 1999): The effect of COD to N ratio on nitrite accumulation during nitrate reduction by an enriched denitrifying culture fed with acetate was investigated. Experiments were carried out in a 10-L sequencing batch reactor (SBR) operated for activated sludge denitrification. At the beginning of the test, 50 mg N/L nitrate and 130 mg COD/L acetated were provided to the reactor. The reduction of nitrate, the accumulation of nitrite and the oxidation of carbon source were measured throughout the experiment. The SBR system was maintained in a temperature-controlled laboratory at 21±2°C. SBR operations were controlled with a programmable timer (ChronTrol, XTseries, San Diego, Calif.). Nitrate, nitrite, and acetate were measured using an ion chromatograph (IC) (DionexModel DX-300, AS-10 column, Dionex Corp., Sunnyvale, Ca-lif.). Nitric oxide and N_2O were not measured in the experiment.

Parameter estimation were performed with AQUASIM for aquatic systems (Reichert et al. 1995). Not all the parameters were identifiable from the experimental data, however, most of them have been well established in previous studies, and therefore they were adopted from literature (Hiatt and Grady 2008, Pan et al. 2013b) (Table 2). For example, since relative high COD concentration were used in all the cases, the affinity constants for carbon source of each step (K_{S1} , K_{S2} , K_{S3} and K_{S4}) in the ASMN model were not identifiable based on the experimental data. Therefore, these parameters were adopted from literature. Similar rules applied for some other literature derived parameter values in both models, as listed in Table 2.

In this work, only parameters that are unique for each model and sensitive to the experimental data (η_{g1}, η_{g2}, η_{g4} for the ASMN model and $r_{COD,\max}$, $K_{Mred,1}$, $K_{Mred,2}$ and $K_{Mred,4}$ for the ASM-ICE model) were calibrated. The calibrated parameter values are presented in Table 2 as well. It should be highlighted that the aim of the modelling work is to verify if various model structures (rather than parameter calibrations) could explain the trend of the experimentally observed denitrification dynamics, because having a solid model structure is a key step towards reliable prediction of denitrification intermediates accumulation.

3. RESULTS

3.1. Evaluation of the Mathematical Models: Case 1

In the first case, the ASMN model and the ASM-ICE model were evaluated based on their abilities in predicting the nitrogen conversion by P. *denitrificans* (N.C.1.B. 8944) (Kucera et al. 1983). The experimental data along with the model predictions are presented in Figure 2, demonstrating the influences of nitrite and N_2O on nitrate reduction.

The experimental observations from batch test Set A are shown in Figure 2-a1 & a2. The nitrate reduction rate significantly decreased from 10.8 mg N/hour in phase 1 when only nitrate was present, to 2.6 mg N/hour in phase 2 with nitrite addition. After the depletion of nitrite, the nitrate reduction rate recovered immediately and almost to its original level in phase 3. Results given by the ASM-ICE model agree well with the experimental nitrate and nitrite profiles (Figure 2-a2). In contrast, the ASMN model failed to predict the dynamic change of nitrate profile although the nitrite profile was reasonably reproduced (Figure 2-a1).

The measured nitrate reduction rates under the four different conditions in batch test Set B (Table 3) are shown in Figure 2-b1 & b2. The experimental results showed that the addition

of other chemicals (nitrite, N_2O and antimycin) significantly influenced the nitrate reduction rate. Specifically, considering the value of the nitrate reduction rate as 100% when only nitrate itself was added, the nitrate reduction rate decreased to 32% after nitrite addition, and to 6% after N_2O addition. However, when N_2O, nitrite and antimycin (a chemical which inhibits nitrite and N_2O reduction) were added together, the nitrate reduction rate increased up to 233%.

The ASMN model completely failed to describe these experimentally observed variations in the nitrate reduction rates, but predicted a constant nitrate reduction rate under all conditions (Figure 2-b1). This clearly indicates that the ASMN model is not able to capture the influence of nitrite and N_2O on nitrate reduction. On the contrary, as shown in Figure 2-b2, the ASM-ICE model successfully predicted the influence of nitrite, N_2O and antimycin on nitrate reduction, with 38% of the nitrate reduction rate left after nitrite addition (in comparison to the 32% experimentally observed), 7% left after N_2O addition (in comparison to the experimental data of 6%). The model also correctly predicted the substantial increase (240% in comparisons to the experimentally observed 233%) in the nitrate reduction rate, when antimycin was used to inhibit nitrite and N_2O reduction.

3.2. Evaluation of the Mathematical Models: Case 2

In the second case, the denitrification dynamics by a full-scale activated sludge fed with acetate was studied by McMurray (2008). The experimental data along with the model predictions are presented in Figure 3. No N_2O accumulation was observed throughout the experiment, and the N_2O concentration predicted by both models was also negligible.

The experimental results showed that nitrate was reduced but nitrite accumulated in the first 0.3 hour. After the depletion of nitrate, nitrite was then reduced (Figure 3-a1 & a2). COD was consumed during nitrate and nitrite reduction (Figure 3-b1 & b2). The N_2 production rate was around 22 mg N/hour when both nitrate and nitrite were present, and increased to around 28 mg N/hour when only nitrite was present (Figure 3-c1 & c2).

The ASMN model captured the trends of nitrate and nitrite reduction (Figure 3-a1), and the trend of acetate consumption (Figure 3-b1). However, the fitting errors between the model predictions and experimental data were relatively large. These errors can be clearly seen in the mismatch between the model-predicted and experimentally observed N_2 production rates (Figure 3-c1). In comparison, the ASM-ICE model successfully reproduced all the nitrogen profiles observed, including the changes in N_2 production rate (Figure 3-a2, b2 & c2).

3.3. Evaluation of the Mathematical Models: Case 3

In the third case, the ASMN model and the ASM-ICE model were evaluated based on their ability to capture the nitrogen conversion dynamics by an enriched denitrifying culture fed with methanol as the carbon source (Pan et al. 2013a). The experimental data along with the model predictions are presented in Figure 4.

In the tests when only one nitrogen oxide species was added, the reduction rate of nitrate (Figure 4-a1 & a2), nitrite (Figure 4-b1 & b2) and N_2O (Figure 4-c1 & c2) was 45, 74 and 370 mg N/(gVSS×h), respectively. However, when nitrate, nitrite and N_2O were added simultaneously (Figure 4-d1 & d2), the reduction rate of all the nitrogen oxides decreased to 19, 39 and 256 mg N/(gVSS×h), respectively (Pan et al. 2013a).

Generally, both the ASMN model and the ASM-ICE model were able to reproduce the nitrate (Figure 4-a1 & a2), nitrite (Figure 4-b1 & b2) and N_2O (Figure 4-c1 & c2) profiles when only one nitrogen oxide species was added. However, the ASMN model failed to reproduce the experimental results when the three nitrogen oxide species were added together (Figure 4-d1). The predicted NO_3^- reduction rate was significantly higher than the predicted NO_2^- reduction rate, being inconsistent with the experimental observation. In addition, the predicted N_2O reduction rate was significantly lower than the experimentally observed N_2O reduction rate. In comparison, the ASM-ICE model reproduced all experimental data reasonably well, with slightly poor fitting for nitrite only (Figure 4-d2).

3.4. Evaluation of the Mathematical Models: Case 4

In Case 4, the ASMN model and the ASM-ICE model were evaluated based on their ability to capture the nitrogen conversions by an enriched denitrifying culture fed with acetate as the carbon source. The experimental data along with the model predictions are presented in Figure 5. Nitrite accumulated from 7 mg N/L to around 34 mg N/L in the batch test, while nitrate reduced from 52 mg N/L to 10 mg N/L and COD concentration reduced from 130 mg COD/L to 5 mg COD/L. As shown in Figure 5-a1 & a2, both models were able to reproduce these experimental trends.

4. DISSCUSSION

4.1. Modelling of intermediates dynamics in denitrification

In this work, the two distinct concepts of four-step denitrification models (ASMN and ASM-ICE) were evaluated for their ability to predict denitrification dynamics in four cases from literature. The results obtained using the ASM-ICE model are in better agreement with the experimental data for all four cases. In contrast, the ASMN model failed to reproduce the

experimental data in Cases 1, 2 and 3, and only succeeded in predicting the experimental observation in Case 4.

The question arising herein is why the two models performed differently. The answer to this question lies in their consideration of the electron competition process, which is reflected by the differences in the structure of the two models. In the ASMN model, there is no specific kinetic equation to describe the carbon oxidation process. Instead, the carbon oxidation kinetics and nitrogen oxides reduction kinetics are directly lumped into each denitrification step. Such a structure disables the model to describe the electron competition process, particularly when the carbon oxidation rate limits the overall denitrification rate through a limiting electron supplying flux. In contrast, the carbon oxidation process (II-R_1) and the nitrogen reduction processes (II-R_2 to II-R_5) are modelled separately in the ASM-ICE model (Table 1). The model is able to predict both the electron supply (determined by carbon oxidation process) and consumption rate (determined by nitrogen reduction process). The relative ability of each denitrification step to compete for electrons was modelled with different affinity constants for reduced carriers ($k_{Mred,1}$, $k_{Mred,2}$, $k_{Mred,3}$, $k_{Mred,4}$).

The advantage of the ASM-ICE model over the ASMN model in describing the electron competition process is strongly supported by Case 1, Case 2 and Case 3 studied. In Case 1, the electron supply rate was the rate limiting process in all the tests. This is evident in the experimental data, which showed that the nitrate reduction rate increased by around 233% when antimycin (which inhibits nitrite reduction and the downstream denitrification steps) was added (Figure 2-b2). The ASM-ICE model revealed that the nitrate reduction step (II-R_2) received more electrons with antimycin blocking the electron flows to the other denitrification steps. Thus a higher nitrate reduction rate (240%) was predicted by the ASM-

ICE model. However, the ASMN model failed to reproduce the changes of the nitrate reduction rate (Figure 2-b1), because the structure of the ASMN model itself failed to describe the electron competition process between the four denitrification steps. In addition, the failure of the ASMN model could not be changed by adding any inhibition terms to the kinetic equations as long as the "direct coupling approach" is applied. For example, it is not possible for the ASMN model to predict the 233% increase in the nitrate reduction rate after the addition of antimycin by adding an inhibition term in the model.

Similar to the pure culture study in Case 1, the study of a full activated sludge in Case 2 and an enriched mixed culture in Case 3 also suggested that the electron competition process significantly affects the denitrification intermediates dynamics. For Case 2, the increase of NO_2^- reduction rate (reflected by the N_2 production rate with no nitric oxide and N_2O accumulation) from 22 mg N/hour to 28 mg N/hour indicates that there was electron competition when NO_2^- and NO_3^- were both present leading to a lower nitrite reduction rate (and N_2 production rate) in this case. The competition between nitrate reduction and nitrite reduction disappeared after the depletion of NO_3^- and therefore a higher nitrite reduction rate was achieved. For Case 3, the decline of the reduction rates of nitrate, nitrite and N_2O when all of them were added was also due to electron competition (Figure 4-d1 & d2). Therefore, the ASM-ICE model gives a better prediction of the case compared to the ASMN model.

Different from the above cases, both models performed equally well in Case 4. A feature in this case is that the availability of electron acceptors did not change throughout the experiment, with the concentrations of both nitrate and nitrite were substantially above the respective affinity constants. Also, the electron donor was also in excess during most of the experimental period. Under such conditions, the electron allocation to different denitrification

399 steps is expected to be constant, which could be adequately captured by both models.
400 However, the predictive ability of ASMN under changed electron acceptor conditions may be
401 questionable, based on the results obtained in Cases 1-3.
402
403 **4.2. Application of the ASM-ICE denitrification model**
404 This work revealed that the ASMN-type model is structurally deficient in describing the
405 electron competition process in denitrification. This is normally not a problem if the model is
406 aimed to predict the overall nitrogen and COD removal performance in a wastewater
407 treatment plant, as in most cases the low level accumulation of denitrification intermediates
408 do not significantly affect the overall nitrogen removal rate. However, in the context of
409 predicting the accumulation of denitrification intermediates, the structure of ASMN is
410 inadequate. For example, the accumulation of N_2O to 0.1 mg N/L in the anoxic zone in a pre-
411 denitrification system, while not having a significant effect on the nitrogen removal
412 performance, could potentially lead to an N_2O emission factor of 1% of the nitrogen load
413 (Pan et al. 2013c). With the increasing use of nitrogen removal by the nitritation pathway (Ni
414 and Yu 2008), the prediction of nitrite accumulation is also becoming more important. In
415 such situations, the concept of the ASM-ICE model should be adopted.
416
417 The application of the ASM-ICE type model requires information on both the carbon
418 oxidation reaction kinetics and the nitrogen reduction kinetics. Due to the lack of
419 understanding of the electron competition process in most of the previous studies, the
420 respective reaction kinetics of the carbon oxidation and nitrogen reduction processes were not
421 well established. For instance, the maximum carbon source oxidation rate ($r_{COD,\max}$), which is
422 the key parameter to restrict the overall model predicted carbon oxidation (electron supply)
423 rate, does not exist in the previous ASMN type of models and therefore is not available in

literature. The electron affinity constant ($K_{Mred,1}$ $K_{Mred,2}$, $K_{Mred,3}$ and $K_{Mred,4}$), which are newly proposed in the ASM-ICE model to replace the affinity constant to carbon source of each denitrification step (K_{S1}, K_{S2}, K_{S3} and K_{S4}) in the ASMN model, are also not available in literature. Therefore, more efforts are needed to provide more information on the key parameters of the ASM-ICE model for its further implementation. In addition, efforts are needed to obtain more information on the reaction kinetics of the nitric oxide reduction. NO is a compulsory intermediate of denitrification but is usually difficult to measure. While the current ASM-ICE model may not yet serve as a precise and quantitative predictor of intermediates accumulation in various wastewater treatment systems (due to parameter value uncertainties), it can nevertheless serve as tool to explore the effect of operational conditions on intermediates dynamics, and its continued testing against more experimental data will serve to confirm the consensus mechanism of electron competition across denitrification systems, and delineate a range/pattern in parameter values. Nitric oxide, which is an inevitable intermediate of denitrification but usually very hard to be measured,

In future work, experiment designs should be optimized to provide more information on the kinetics of both the carbon oxidation and the nitrogen reduction processes from different cultures/sludges and under different conditions. The parameters obtained with different experiments and cultures should then be compared and synthetised, aiming at form a consistent pattern which could then be implemented as default values of the parameters of the ASM-ICE model for practical applications. Further improvement/simplification of the ASM-ICE model structure might be achieved depending on the new parameter pattern and the model performance. A fully calibrated and verified ASM-ICE model is expected to provide strong support to both future experimental studies and modelling practice aiming at get better understanding of biological denitrification in wastewater treatment.

5. CONCLUSIONS

In this work, two distinct mathematical model structures for denitrification were compared for their ability to predict nitrogen conversion dynamics in one pure culture and three mixed culture studies. It was demonstrated that the ASM-ICE model was able to describe the experimental data in all four cases studied; however, the ASMN model failed to describe the experimental data from three cases. The results suggest that the ASM-ICE model is advantageous over the ASMN model in describing the electron competition between the four steps of denitrification and in predicting the accumulation of denitrification intermediates. The ASM-ICE model is expected to provide strong support to both future experimental studies and modelling practice aiming at get better understanding of biological denitrification in wastewater treatment.

ACKNOWLDEGEMENT

This study was funded by the Australian Research Council, Western Australia Water Corporation and Melbourne Water Corporation through projects LP0991765 and DP0987204. Bing-Jie Ni acknowledges the support of Australian Research Council Discovery Early Career Researcher Award (DE130100451).

REFERENCES

Zumft, W.G. (1997) Cell biology and molecular basis of denitrification. Microbiology and Molecular Biology Reviews 61(4), 533-616.

Tchobanoglous, G., Burton, F. and Stensel, H.D. (2003) Wastewater engineering: treatment and reuse, Metcalf & Eddy, Inc., McGraw Hill Education, New York.

Ni, B.-J. and Yu, H.-Q. (2008) An approach for modeling two-step denitrification in activated sludge systems. Chemical Engineering Science 63(6), 1449-1459.

IPCC (2007) Climate Change 2007: The Physical Science Basis. Contribution of Working Group I to the Fourth Assessment Report of the Intergovernmental Panel on Climate Change [Solomon, S., D. Qin,

M. Manning, Z. Chen, M. Marquis, K.B. Averyt, M. Tignor and H.L. Miller (eds.)]. Cambridge University Press, Cambridge, United Kingdom and New York, NY, USA.
Ravishankara, A.R., Daniel, J.S. and Portmann, R.W. (2009) Nitrous oxide (N_2O): The dominant ozone-depleting substance emitted in the 21st century. Science 326(5949), 123-125.
Pan, Y., Ni, B.-J., Bond, P.L., Ye, L. and Yuan, Z. (2013a) Electron competition among nitrogen oxides reduction during methanol-utilizing denitrification in wastewater treatment. Water Research 47(10), 3273-3281.
Schalk-Otte, S., Seviour, R.J., Kuenen, J.G. and Jetten, M.S.M. (2000) Nitrous oxide (N_2O) production by *Alcaligenes faecalis* during feast and famine regimes. Water Research 34(7), 2080-2088.
Richardson, D., Felgate, H., Watmough, N., Thomson, A. and Baggs, E. (2009) Mitigating release of the potent greenhouse gas N_2O from the nitrogen cycle - could enzymic regulation hold the key? Trends in Biotechnology 27(7), 388-397.
Henze, M., Gujer, W., Mino, T. and van Loosdrecht, M.C.M. (2000) Activated sludge models ASM1, ASM2, ASM2d, and ASM3, IWA Scientific and Technical Report No. 9. IWA Publishing, London, UK.
Ni, B.-J., Ruscalleda, M., Pellicer-Nàcher, C. and Smets, B.F. (2011) Modeling nitrous oxide production during biological nitrogen removal via nitrification and denitrification: extensions to the general ASM models. Environmental Science & Technology 45(18), 7768-7776.
Vonschulthess, R., Wild, D. and Gujer, W. (1994) Nitric and nitrous oxides from denitrifying activated-sludge at low-oxygen concentration. Water Science and Technology 30(6), 123-132.
Schulthess, R.V. and Gujer, W. (1996) Release of nitrous oxide (N_2O) from denitrifying activated sludge: Verification and application of a mathematical model. Water Research 30(3), 521-530.
Hiatt, W.C. and Grady, C.P.L. (2008) An updated process model for carbon oxidation, nitrification, and denitrification. Water Environment Research 80(11), 2145-2156.
Pan, Y., Ni, B.-J. and Yuan, Z. (2013b) Modeling electron competition among nitrogen oxides reduction and N_2O accumulation in denitrification. Environmental Science & Technology 47(19), 11083-11091.
Kucera, I., Dadak, V. and Dobry, R. (1983) The distribution of redox equivalents in the anaerobic respiratory chain of *paracoccus* denitrificans. European Journal of Biochemistry 130(2), 359-364.
Pan, Y., Ye, L., Ni, B.-J. and Yuan, Z. (2012) Effect of pH on N_2O reduction and accumulation during denitrification by methanol utilizing denitrifiers. Water Research 46(15), 4832-4840.
McMurray, S.H. (2008) Formation of denitrification intermediates and their impact on process performance. PhD Thesis, The University of Queensland, Brisbane, Australia.
Oh, J. and Silverstein, J. (1999) Acetate limitation and nitrite accumulation during denitrification. Journal of Environmental Engineering-Asce 125(3), 234-242.
Reichert, P., von Schulthess, R. and Wild, D. (1995) The use of AQUASIM for estimating parameters of activated sludge models. Water Science and Technology 31(2), 135-147.
Pan, Y., Ye, L. and Yuan, Z. (2013c) Effect of H_2S on N_2O reduction and accumulation during denitrification by methanol utilizing denitrifiers. Environmental Science & Technology 47(15), 8408-8415.

Table 1: Process matrices for the two types of denitrification models evaluated in this study

Processes	Model components									Kinetic rate expressions
	S_{NO3}	S_{NO2}	S_{NO}	S_{N2O}	S_{N2}	S_S	S_{Mox}	S_{Mred}	X	
Model I (ASMN)- the "direct coupling appraoch" adapted from Hiatt and Grady (2008)										
I-R_1	-A	+A				$-1/(Y_H \cdot \eta_Y)$			1	$R1 = \mu_H \cdot \eta_{g1} \cdot X(\frac{S_S}{K_{S1}+S_S})(\frac{S_{NO3}}{K_{NO3}^{HB}+S_{NO3}})$
I-R_2		-B	+B			$-1/(Y_H \cdot \eta_Y)$			1	$R2 = \mu_H \cdot \eta_{g2} \cdot X(\frac{S_S}{K_{S2}+S_S})(\frac{S_{NO2}}{K_{NO2}^{HB}+S_{NO2}})(\frac{K_{NO,2}}{K_{NO,2}+S_{NO}})$
I-R_3			-B	+B		$-1/(Y_H \cdot \eta_Y)$			1	$R3 = \mu_H \cdot \eta_{g3} \cdot X(\frac{S_S}{K_{S3}+S_S})(\frac{S_{NO}}{K_{NO}^{HB}+S_{NO}+S_{NO}^2/K_{NO,3}})$
I-R_4				-B	+B	$-1/(Y_H \cdot \eta_Y)$			1	$R2 = \mu_H \cdot \eta_{g4} \cdot X(\frac{S_S}{K_{S4}+S_S})(\frac{S_{N2O}}{K_{N2O}^{HB}+S_{N2O}})(\frac{K_{NO,4}}{K_{NO,4}+S_{NO}})$
Model II (ASM-ICE)- the "indirect coupling approach" adapted from Pan et al.(2013b)										
II-R_1						-1	$-(1-Y_H)$	$1-Y_H$	Y_H	$R1 = r_{COD,\max} X(\frac{S_S}{K_S+S_S})(\frac{S_{Mox}}{K_{Mox}+S_{Mox}})$
II-R_2	-1	1					1	-1		$R2 = r_{NO3,\max} X(\frac{S_{NO3}}{K_{NO3}^{HB}+S_{NO3}})(\frac{S_{Mred}}{K_{Mred,1}+S_{Mred}})$
II-R_3		-1	1				$\frac{1}{2}$	$-\frac{1}{2}$		$R3 = r_{NO2,\max} X(\frac{S_{NO2}}{K_{NO2}^{HB}+S_{NO2}})(\frac{S_{Mred}}{K_{Mred,2}+S_{Mred}})$
II-R_4			-1	$\frac{1}{2}$			$\frac{1}{2}$	$-\frac{1}{2}$		$R4 = r_{NO,\max} X(\frac{S_{NO}}{K_{NO}^{HB}+S_{NO}})(\frac{S_{Mred}}{K_{Mred,3}+S_{Mred}})$
II-R_5				-1	1		1	-1		$R5 = r_{N2O,\max} X(\frac{S_{N2O}}{K_{N2O}^{HB}+S_{N2O}})(\frac{S_{Mred}}{K_{Mred,4}+S_{Mred}})$

A= $\frac{1-Y_H \cdot \eta_Y}{1.143 \cdot Y_H \cdot \eta_Y}$, B= $\frac{1-Y_H \cdot \eta_Y}{0.571 \cdot Y_H \cdot \eta_Y}$, $S_{Mred} + S_{Mox} = C_{tot}$

521 **Table 2:** Best-fit parameters of the two models describing denitrification dynamics

Parameter	Definition	Case 1	Case 2	Case 3	Case 4	Source
Model I (ASMN)- the "direct coupling appraoch" adapted from Hiatt and Grady (2008)						
μ_H	Maximum specific growth rate (hour^{-1})	0.26	0.26	0.26	0.26	Hiatt and Grady (2008)
Y_H	Heterotrophic yield (g COD/g COD)	0.6[a]	0.6[a]	0.5[b]	0.6[a]	a: Hiatt and Grady (2008) b: Pan et al. (2013b)
η_Y	Anoxic yield factor (dimensionless)	0.9	0.9	0.9	0.9	Hiatt and Grady (2008)
η_{g1}	Anoxic growth factor, R1 (dimensionless)	0.029	0.14	0.18	0.14	Estimated
η_{g2}	Anoxic growth factor, R2 (dimensionless)	0.024	0.058	0.15	0.016	Estimate
η_{g3}	Anoxic growth factor, R3 (dimensionless)	0.35	0.35	0.35	0.35	Hiatt and Grady (2008)
η_{g4}	Anoxic growth factor, R4 (dimensionless)	0.35[a]	0.35[a]	0.81[b]	0.35[a]	a: Hiatt and Grady (2008) b: Estimated
K_{S1}	Affinity constant for Ss, R1 (mgCOD/L)	20	20	20	20	Hiatt and Grady (2008)
K_{S2}	Affinity constant for Ss, R2 (mgCOD/L)	20	20	20	20	Hiatt and Grady (2008)
K_{S3}	Affinity constant for Ss, R3 (mgCOD/L)	20	20	20	20	Hiatt and Grady (2008)
K_{S4}	Affinity constant for Ss, R4 (mgCOD/L)	40	40	40	40	Hiatt and Grady (2008)
K_{NO3}^{HB}	Affinity constant for nitrate-nitrogen (mg N/L)	0.2	0.2	0.2	0.2	Hiatt and Grady (2008)
K_{NO2}^{HB}	Affinity constant for nitrite-nitrogen (mg N/L)	0.2	0.2	0.2	0.2	Hiatt and Grady (2008)
K_{NO}^{HB}	Affinity constant for nitric oxide-nitrogen (mg N/L)	0.05	0.05	0.05	0.05	Hiatt and Grady (2008)
K_{N2O}^{HB}	Affinity constant for nitrous oxide-nitrogen (mg N/L)	0.05	0.05	0.05	0.05	Hiatt and Grady (2008)
$K_{NO,2}$	NO inhibition coefficient, R2 (mg N/L)	0.5	0.5	0.5	0.5	Hiatt and Grady (2008)
$K_{NO,3}$	NO inhibition coefficient, R3 (mg N/L)	0.3	0.3	0.3	0.3	Hiatt and Grady (2008)
$K_{NO,4}$	NO inhibition coefficient, R4 (mg N/L)	0.075	0.075	0.075	0.075	Hiatt and Grady (2008)
Model II (ASM-ICE)- the "indirect coupling approach" adapted from Pan et al.(2013b)						
$r_{COD,\max}$	Maximum carbon source oxidation rate (mmol COD/(L*hour)	0.064	0.090	0.34	0.129	Estimated

$r_{NO3,\max}$	Maximum nitrate reduction rate (mmol NO_3^- /mmol biomass*hour)	0.045	0.045	0.045	0.045	Pan et al. (2013b)
$r_{NO2,\max}$	Maximum nitrite reduction rate (mmol NO_2^- /mmol biomass*hour)	0.059	0.059	0.059	0.059	Pan et al. (2013b)
$r_{NO,\max}$	Maximum nitric oxide reaction rate (mmol NO /mmol biomass*hour)	0.56	0.56	0.56	0.56	Pan et al. (2013b)
$r_{N2O,\max}$	Maximum nitrous oxide reaction rate (mmol N_2O /mmol biomass*hour)	0.23	0.23	0.23	0.23	Pan et al. (2013b)
K_S	Affinity constant for Ss (mmol COD/L)	0.1	0.1	0.1	0.1	Pan et al. (2013b)
K_{NO3}^{HB}	Affinity constant for nitrate-nitrogen (mmol NO_3^- /L)	0.018	0.018	0.018	0.018	Pan et al. (2013b)
K_{NO2}^{HB}	Affinity constant for nitrite-nitrogen (mmol NO_2^- /L)	0.0041	0.0041	0.0041	0.0041	Pan et al. (2013b)
K_{NO}^{HB}	Affinity constant for nitric oxide-nitrogen (mmol NO/L)	0.000011	0.000011	0.000011	0.000011	Pan et al. (2013b)
K_{N2O}^{HB}	Affinity constant for nitrous oxide-nitrogen (mmol N_2O/L)	0.0025	0.0025	0.0025	0.0025	Pan et al. (2013b)
K_{Mox}	Affinity constant for S_{Mox}, R1 mmol/(mmol biomass)	0.0001	0.0001	0.0001	0.0001	Pan et al. (2013b)
$K_{Mred,1}$	Affinity constant for S_{Mred}, R2	0.0015[a]	0.0068[a]	0.0046[b]	0.0018[a]	a:Estimated b: Pan et al. (2013b)
$K_{Mred,2}$	Affinity constant for S_{Mred}, R3	0.00058[a]	0.016[a]	0.00040[b]	0.0033[a]	a:Estimated b: Pan et al. (2013b)
$K_{Mred,3}$	Affinity constant for S_{Mred}, R4	0.000010	0.000010	0.000010	0.000010	Pan et al. (2013b)
$K_{Mred,4}$	Affinity constant for S_{Mred}, R5	0.00024[a]	0.0032[b]	0.0032 [b]	0.0032 [b]	a: Estimated b: Pan et al. (2013b)
Y_H	Heterotrophic yield	0.6[a]	0.6[a]	0.5[b]	0.6[a]	a: Hiatt and Grady (2008) b: Pan et al. (2013b)
C_{tot}	Total electron carrier concentration mmol/mmol biomass	0.01	0.01	0.01	0.01	Pan et al. (2013b)

522

523

524 **Table 3: Four experimental cases used for evaluation of the two denitrification models**

	Culture	Carbon source	Nitrogen oxides added	Batch tests
Case 1	pure denitrifying culture	glucose	NO_3^-, NO_2^- N_2O and antimycin	a) the effect of nitrite addition on nitrate reduction, b) the impact of nitrite, N_2O or antimycin on nitrate reduction rate
Case 2	full-scale activated sludge	acetate	NO_3^-, NO_2^-	the relationship between nitrate and nitrite reduction, acetate oxidation and nitrogen gas production
Case 3	enriched denitrifying culture	methanol	NO_3^-, NO_2^-, N_2O	1) NO_3^- reduction with only NO_3^- being added 2) NO_2^- reduction with only NO_2^- being added 3) N_2O reduction with only N_2O being added 4) NO_3^- , NO_2^- and N_2O reduction with NO_3^-, NO_2^- and N_2O being added simultaneously
Case 4	enriched denitrifying culture	acetate	NO_3^-	Investigating the nitrite accumulation during nitrate reduction

525

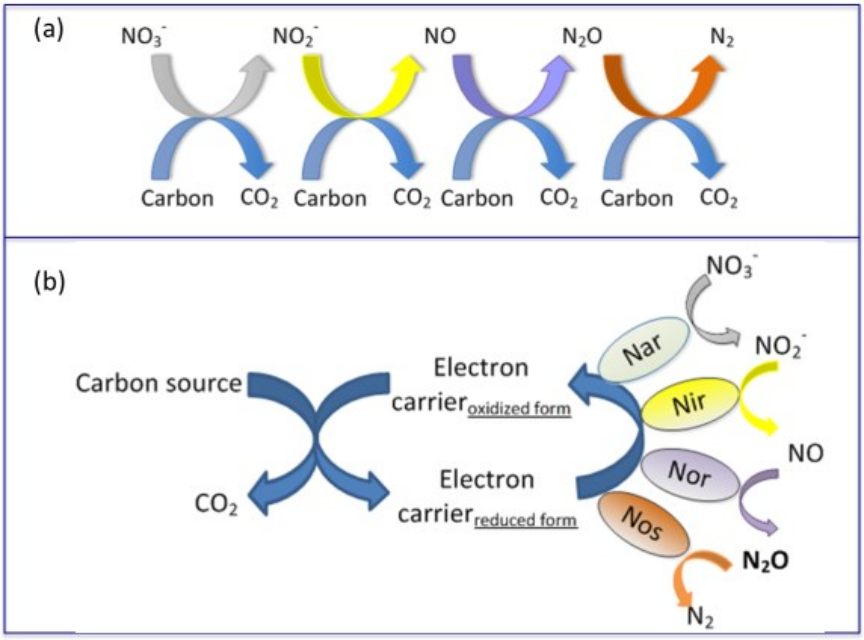

526

527 **Figure 1.** Conceptual reaction schemes used in the two 4-step denitrification models
528 evaluated in this study: (a) The ASMN model - Using the "direct coupling approach" to
529 model the carbon oxidation and nitrogen reduction processes during denitrification; (b) The
530 ASM-ICE model - Using the "*indirect coupling approach*" to model the carbon oxidation and
531 nitrogen reduction processes during denitrification.

532

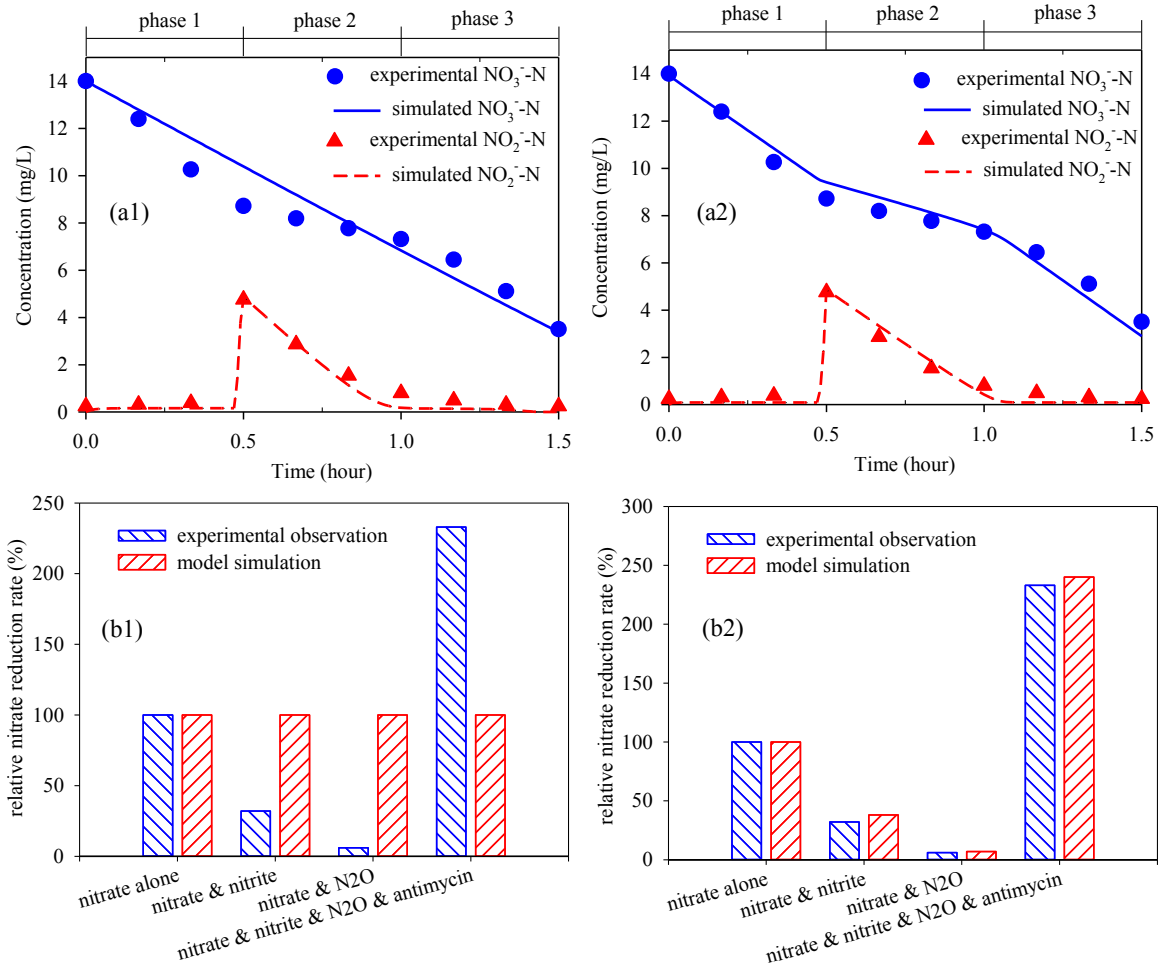

533

534 **Figure 2:** Experimental results and model predictions for Case 1 (Kucera et al. 1983). (a1) &

535 (b1) – Evaluation of ASMN; (a2) & (b2) – Evaluation of ASM-ICE.

536

537

538

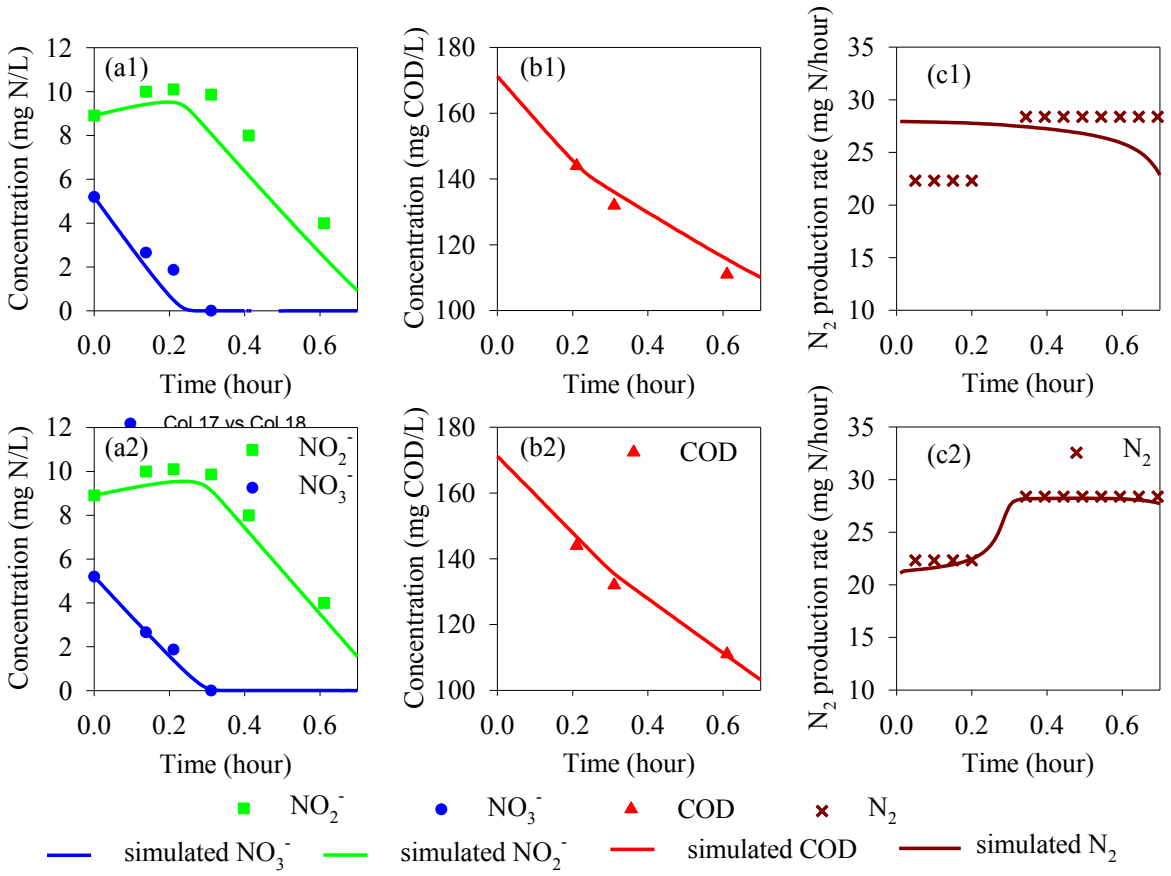

539

540 **Figure 3:** Experimental results and model predictions in Case 2 (McMurray 2008): (a1), (b1)
541 & (c1) - Evaluation of ASMN; (a2), (b2) & (c2) - Evaluation of ASM-ICE (the model
542 simulations are shown in lines).

543

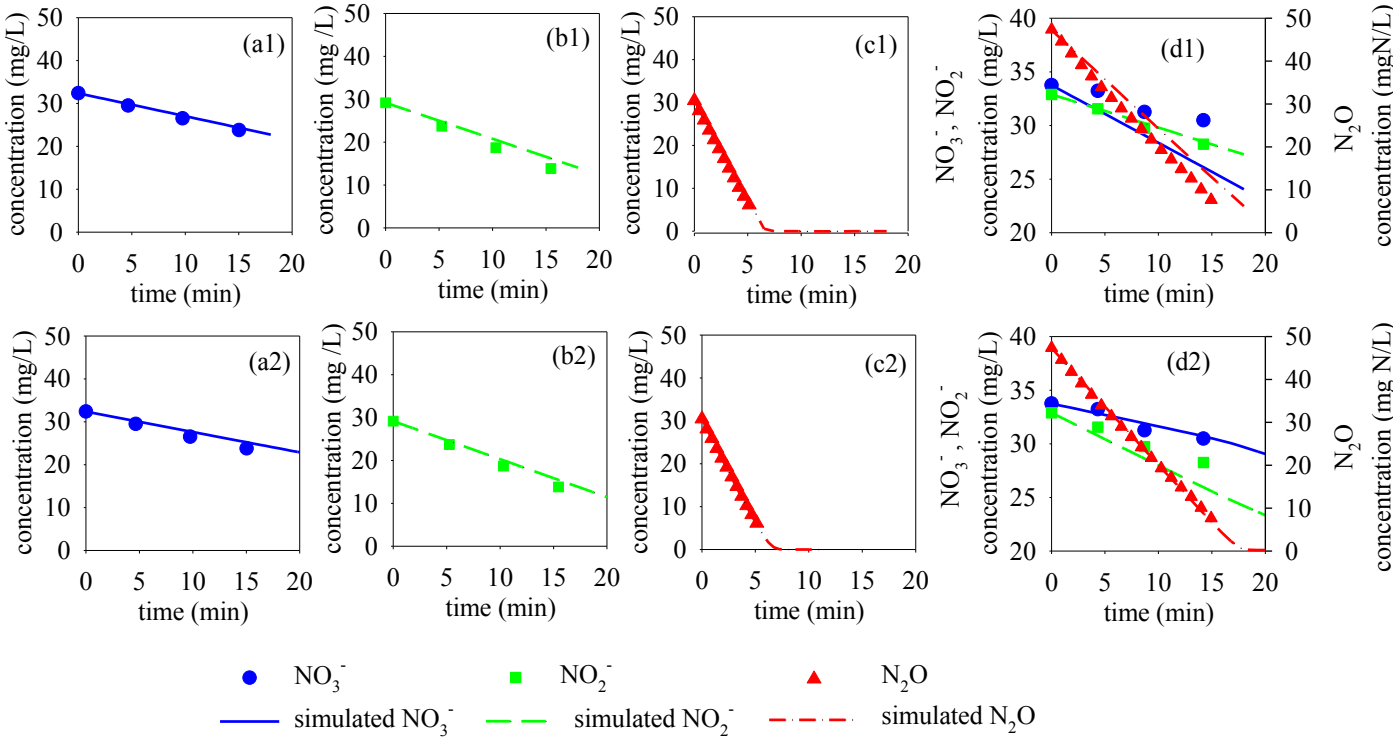

544

545 **Figure 4:** Experimental results and model predictions in Case 3 (Pan et al. 2013a): (a1) & (b1)

546 & (c1) & (d1) - Evaluation of ASMN; (a2) & (b2) & (c2) & (d2) - Evaluation of ASM-ICE.

547

548

549

550

551

552

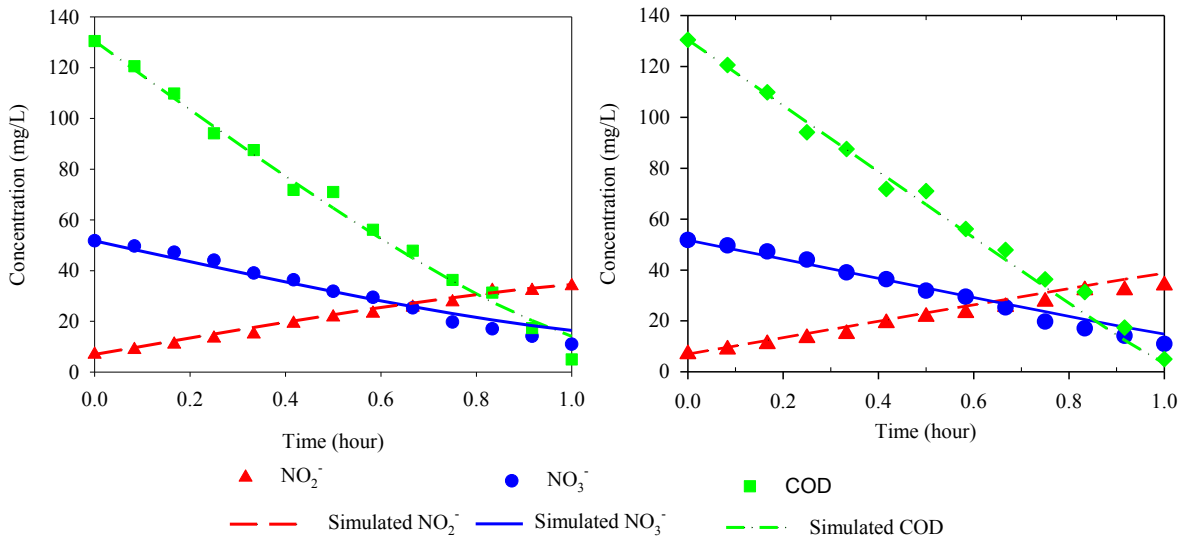

553

554 **Figure 5:** Experimental results and model predictions in Case 4 (Oh and Silverstein 1999):

555 (a1) & (b1) & (c1) & (d1) - Evaluation of ASMN; (a2) & (b2) & (c2) & (d2) - Evaluation of

556 ASM-ICE.

557

558

559